

First measurement of the helicity asymmetry for $\gamma p \rightarrow p\pi^0$ in the resonance region

M. Gottschall¹, A.V. Anisovich^{1,5}, B. Bantes², D. Bayadilov^{1,5}, R. Beck¹, M. Bichow⁶, S. Böse¹, K.-Th. Brinkmann^{1,3}, Th. Challand⁴, V. Crede⁷, F. Dietz³, H. Dutz², H. Eberhardt², D. Elsner², R. Ewald², K. Fornet-Ponse², St. Friedrich³, F. Frommberger², Ch. Funke¹, A. Gridnev⁵, M. Grüner¹, E. Gutz^{1,3}, Ch. Hammann¹, J. Hannappel², J. Hartmann¹, W. Hillert², Ph. Hoffmeister¹, Ch. Honisch¹, I. Jaegle⁴, D. Kaiser¹, H. Kalinowsky¹, S. Kammer², I. Keshelashvili⁴, F. Klein², E. Klempt¹, K. Koop¹, B. Krusche⁴, M. Kube¹, M. Lang¹, I. Lopatin⁵, Y. Maghrbi⁴, K. Makonyi³, V. Metag³, W. Meyer⁶, J. Müller¹, M. Nanova³, V. Nikonov^{1,5}, R. Novotny³, D. Piontek¹, G. Reicherz⁶, T. Rostomyan¹, A. Sarantsev^{1,5}, St. Schaepe¹, Ch. Schmidt¹, H. Schmieden², R. Schmitz¹, T. Seifen¹, V. Sokhoyan¹, A. Thiel¹, U. Thoma¹, M. Urban¹, H. van Pee¹, D. Walther¹, Ch. Wendel¹, U. Wiedner⁶, A. Wilson⁷, and A. Winnebeck¹.

(The CBELSA/TAPS Collaboration)

¹*Helmholtz-Institut für Strahlen- und Kernphysik, Universität Bonn, Germany*

²*Physikalisches Institut, Universität Bonn, Germany*

³*II. Physikalisches Institut, Universität Gießen, Germany*

⁴*Physikalisches Institut, Universität Basel, Switzerland*

⁵*Petersburg Nuclear Physics Institute, Gatchina, Russia*

⁶*Institut für Experimentalphysik I, Ruhr-Universität Bochum, Germany*

⁷*Department of Physics, Florida State University, Tallahassee, FL 32306, USA*

(Dated: April 16, 2018)

The first measurement of the helicity dependence of the photoproduction cross section of single neutral pions off protons is reported for photon energies from 600 to 2300 MeV, covering nearly the full solid angle. The data are compared to predictions from the SAID, MAID, and BnGa partial wave analyses. Strikingly large differences between data and predictions are observed which are traced to differences in the helicity amplitudes of well known and established resonances. Precise values for the helicity amplitudes of several resonances are reported.

PACS numbers:

The spin structure of the proton has been of topical interest since the discovery that the quark spins constitute an unexpectedly small fraction of the proton spin [1]. Deep inelastic scattering experiments have revealed gluonic contributions to the proton spin to be consistent with zero, at least within the admittedly large errors [2]. At low energies, a different aspect of the proton spin structure is tested by a comparison of the helicity dependence of the total γp cross section integrated over all photon energies, $\int_0^\infty dE_\gamma (\sigma_{3/2} - \sigma_{1/2})/E_\gamma$, with the proton magnetic moment [3], a relation which is known as Gerasimov-Drell-Hearn (GDH) sum rule [4, 5]. The subscripts denote the total helicity, $h=1/2$ for photon and proton spin anti-aligned, $h=3/2$ for both spins aligned. The GDH integral sums over all energies and all final states. A breakdown of the GDH integral into exclusive final states can provide a link between inclusive properties of the proton like its magnetic moment and the contributions of specific nucleon resonances to the GDH integral.

In this letter, we report the first measurement of the double polarization observable

$$E = \frac{\left(\frac{d\sigma}{d\Omega}\right)_{1/2} - \left(\frac{d\sigma}{d\Omega}\right)_{3/2}}{\left(\frac{d\sigma}{d\Omega}\right)_{1/2} + \left(\frac{d\sigma}{d\Omega}\right)_{3/2}} \quad (1)$$

for the exclusive reaction $\gamma p \rightarrow p\pi^0$ in the energy range

from 600 to 2300 MeV, and compare the results with predictions of well established partial wave analyses (PWA) like SAID [6, 7], MAID [8], and BnGa [9]. The double polarization observable G [10] – governing the correlation between linearly polarized photons and longitudinally polarized target protons – revealed remarkable differences in the predictions of the three partial wave analysis groups even in the well-studied 2nd resonance region around $E_\gamma = 750$ MeV [11]. Here, we extend the covered energy regime to 2.3 GeV for the double polarization observable E . So far, data on E were published up to 780 MeV for a limited angular range [12, 13]; further data from CLAS exist and were reported at a conference [14].

The experiment was carried out using the tagged photon beam of the ELection Stretcher Accelerator ELSA at Bonn [15]. Photons with circular polarization [16],

$$P_\odot = \frac{4x - x^2}{4 - 4x + 3x^2} P_{e^-} \quad \text{with } x = \frac{E_\gamma}{E_{e^-}}, \quad (2)$$

were produced by scattering a 2.4 GeV beam of longitudinally polarized electrons with polarization P_{e^-} off a bremsstrahlung target. The electrons were deflected by a magnet into a tagging hodoscope which defines the energy of the bremsstrahlung photons. The electron polarization ($P_{e^-} \approx 0.60$) was monitored in a Møller polarimeter [17]. The photon beam impinged on a butanol (C_4H_9OH) target, which was polarized by dynamic

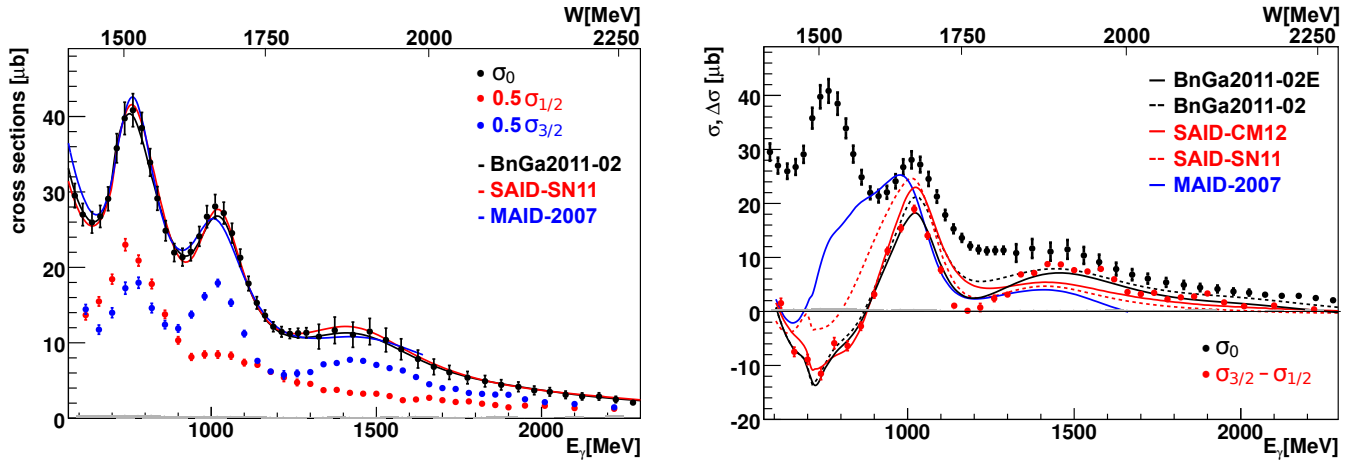


Figure 1: The total cross section σ_0 [28] plotted together with its two helicity components (left) and $\sigma_{3/2} - \sigma_{1/2}$ (right) as a function of E_γ . The error bars give the statistical errors, the systematic errors are shown as a dark gray band.

nucleon polarization [18]. An average polarization of $P_T \approx 0.71$ was obtained.

Particles produced by photoproduction off the target were detected in a 4π geometry using several sub-detectors. The target was surrounded by an inner scintillating fiber detector designed to detect charged particles [19], and by the CsI(Tl) Crystal Barrel detector [20]. A forward calorimeter of 90 CsI(Tl) crystals and a TAPS wall of 216 BaF₂ crystals [21] completed the calorimeter setup in the forward direction. For charged particle detection, both forward calorimeters were equipped with plastic scintillation counters in front of the crystals. With this setup, the four-momenta of neutral mesons decaying into photons could be determined by measuring their energies and directions from the target center to the shower center. The reaction $\gamma p \rightarrow p\pi^0 \rightarrow p\gamma\gamma$ was reconstructed by a series of kinematic cuts. Events with exactly two photons and a proton were used. The latter was demanded in order to suppress background from reactions off neutrons. For the proton candidate, only a hit in one of the charged particle detectors was required to include also low energy protons, which did not reach the calorimeter. The invariant mass of the two photons and the missing mass was calculated and a $\pm 2\sigma$ cut around the π^0 and the proton mass was applied. The azimuthal angle between the direction of proton and meson was asked to be 180° within a $\pm 2\sigma$ window (coplanarity). To remove untagged events originating from photons below the tagging threshold (due to random coincidences), the beam photon energy was also calculated from the reaction and compared to the measured photon energy. Finally, a time coincidence was required between the tagger hit and the reaction products and random time background was subtracted.

The helicity-dependent differential cross section for photoproduction of neutral pions off longitudinally po-

larized protons can be written as

$$\frac{d\sigma}{d\Omega} = \frac{d\sigma_0}{d\Omega} (1 \pm P_T P_\odot E). \quad (3)$$

When a butanol (C₄H₉OH) target is used, unpolarized (u) free protons (f) as well as nucleons bound (b) in carbon or oxygen contribute to the count rate, in addition to the polarized (p) free protons. For the same number of beam photons for both photon helicities, and under the assumption that (unpolarized) nucleons bound in carbon have the same response to impinging photons as nucleons bound in oxygen, we get for beam and target polarized in the same direction the yield $N_{3/2} = N_{3/2}^{f,p} + N^{f,u} + N^b$ and in opposite direction $N_{1/2} = N_{1/2}^{f,p} + N^{f,u} + N^b$, which leads to

$$E = \frac{N_{1/2} - N_{3/2}}{N_{1/2} + N_{3/2}} \cdot \frac{1}{d} \cdot \frac{1}{P_\odot P_T}. \quad (4)$$

The bound nucleons are taken into account by the dilution factor $d = \frac{N^f}{N^f + N^b}$. It was determined by an additional measurement using a carbon foam target with approximately the same density, size, and environment as the carbon and oxygen part of the butanol target. The fraction of carbon (and oxygen) in butanol was then determined using two alternative methods [22]: by fitting a) the missing mass and b) the coplanarity distribution outside of the signal of the free protons. The resulting scaling factor $s(E_\gamma)$ for each energy bin was then used to determine

$$d(E_\gamma, \theta_\pi) = \frac{N_{C_4H_9OH}(E_\gamma, \theta_\pi) - s(E_\gamma) \cdot N_C(E_\gamma, \theta_\pi)}{N_{C_4H_9OH}(E_\gamma, \theta_\pi)}. \quad (5)$$

Fig. 1 shows on the left the total cross section σ_0 and its decomposition into the two helicity components $\sigma_0 = 1/2(\sigma_{1/2} + \sigma_{3/2})$. The latter cross sections were calculated from the values for E reported below - and

extrapolated into the unmeasured angular bins by the BnGa-PWA - and the total cross section σ_0 (from the BnGa-PWA). The figure reveals important details of the spin structure of the photo-excitation of the proton; $\sigma_{1/2}$ and $\sigma_{3/2}$ evidence quite different structures. Both cross sections show a peak at $W \approx 1500$ MeV in $\sigma_{1/2}$ and, slightly shifted, at $W \approx 1520$ MeV in $\sigma_{3/2}$. The latter peak can be assigned to the $N(1520)3/2^-$ and its large helicity coupling to $h=3/2$. The lower mass peak cannot be solely due to the $N(1535)1/2^-$: contributions from other resonances or from background amplitudes, e.g. in the $1/2^-$ partial wave, must be significant. The $N(1680)5/2^+$ contributes nearly only to $\sigma_{3/2}$, where a clear peaking structure is observed. A broad structure at $W \approx 1900$ MeV is very visible in the $\sigma_{3/2}$ excitation curve and seems to be absent in $\sigma_{1/2}$. Photons in the $E_\gamma \approx 1500$ MeV range may excite some of the resonances with spin $J = 1/2, \dots, 7/2$ in the $W = 1900-2000$ MeV mass region. Their contribution is also well visible in the cross section difference $\sigma_{3/2} - \sigma_{1/2} = -E \cdot 2\sigma$ in Fig. 1 on the right. Obviously, they are preferentially excited by the $A_{3/2}$ helicity amplitude.

The helicity asymmetry E in eq.(4) is a function of the pion production angle θ_π . Fig. 2 shows selected results. There are very significant changes in these distributions as a function of energy. Obviously, the quantity E is very sensitive to the contributions from baryon resonances. The lowest incident photon energy bin covers the part of the region with positive E . The shape indicates a strong contribution from the $J^P = 1/2^-$ and $J^P = 3/2^-$ partial waves, with $N(1535)1/2^-$ and $N(1520)3/2^-$ being the dominant resonances in this energy range. The asymmetry in the angular distribution reflects the presence of several weakly contributing resonances, like $N(1440)1/2^+$ and $\Delta(1232)3/2^+$. The next bin, $E_\gamma = 960-1100$ MeV, covers $N(1680)5/2^+$. Together with the $J^P = 1/2^-$ partial wave, it produces a W-shaped angular distribution. The strong forward-backward asymmetry signals contributions from other partial waves, among which the D_{33} partial wave including the $\Delta(1700)3/2^-$ plays an important role. We have split the 4th resonance region from 1350 to 1650 MeV into three 100 MeV slices. The basic structure remains over the full energy range, which suggests a sizeable contribution from a $J^P = 7/2^+$ resonance, which would lead to a three minima structure in the angular distribution. There are only relatively small differences when the three energy bins are compared: $\Delta(1950)7/2^+$ seems to be the dominant contribution. The highest mass bin exhibits strong structures but no clear pattern; several resonances seem to make comparable contributions to the data.

Next we compare the data in Figs. 1 and 2 with predictions from SAID (SN11 and CM12 [6, 7]), MAID [8] and BnGa2011-02 [9]. In addition, a fit to the data within the BnGa-PWA (BnGa2011-02E) is shown. First we note that all PWAs give a reasonable description of $\sigma^{\gamma p \rightarrow p\pi^0}$.

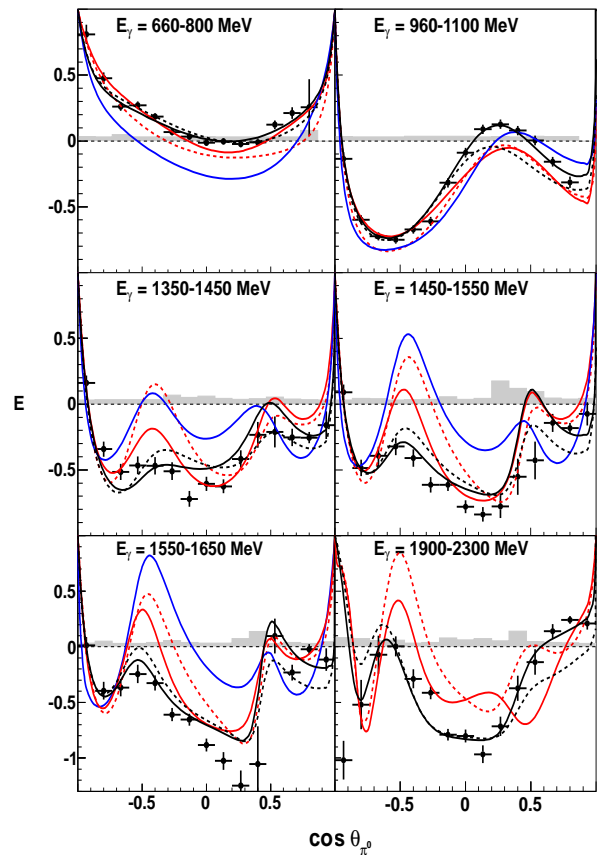


Figure 2: The helicity asymmetry E as a function of $\cos\theta_\pi$ for selected E_γ bins. PWA predictions: black dashed curve: BnGa2011-02, blue solid curve: MAID, red solid curve: CM12, red dashed curve: SN11. Fit to the data points (BnGa2011-02E): black solid curve.

But we find large and unexpected discrepancies already at rather low energies, in the region of the four-star resonances $N(1440)1/2^+$, $N(1535)1/2^-$ and $N(1520)3/2^-$. In the $\Delta(1950)7/2^+$ region, MAID and SAID show a striking enhancement at $\cos\theta_\pi \approx -0.45$. In the MAID online version, the enhancement disappears when the helicity couplings of the $N(1520)3/2^-$ are reduced by a factor of 4. The $N(1520)3/2^-$, however, is the only resonance in this partial wave; hence, such a large effect, which is presumably due to interference with other partial waves, is unexpected. In SN11, this structure is smaller than in MAID, and is further reduced in CM12. The origin of the structure, also visible in the SAID prediction, remains unclear. None of the fits reproduces the data over the full angular range. However, BnGa2011-02 required only a slight adjustment of free parameters to get close to the data points (solution BnGa2011-02E). For examples see Table I. It compares selected results on low-mass excitations of the nucleon for MAID and for the two latest solutions from SAID and BnGa, respectively. One formal difference is remarkable between MAID and SAID

	MAID2007	SN11	CM12	BnGa2011	BnGa2011E		MAID2007	SN11	CM12	BnGa2011	BnGa2011E
N(1440)						N(1520)					
M	1440	1485	1485	1430±8	1430±8		1530	1515	1515±3	1517±3	1516±2
Γ	350	284	284	365±35	360±30		130	104	104±5	114±5	113±5
BR(Nπ)	70	79	79	62±3	62±3		60	63	63±3	62±3	62±2
A _{1/2}	-61	-58±1	-56±1	-61±6	-62±8		-27	-16±2	-19±2	-22±4	-20±3
A _{3/2}							161	156±2	141±2	131±10	131±7
N(1535)						N(1650)					
M	1535	1547	1547	1519±5	1518±4		1690	1635	1635	1651±6	1651±6
Γ	100	188	188	128±14	125±10		100	115	115	104±10	102±10
BR(Nπ)	40	36	36	54±5	55±5		85	100	100	51±4	50±4
A _{1/2}	66	99±2	128±4	105±10	105±9		33	65±25	55±30	33±7	33±7
Δ(1620)						Δ(1950)					
M	1620	1615	1615	1600±8	1598±6		1945	1921	1921	1915±6	1915±5
Γ	150	147	147	130±11	130±8		280	271	271	246±10	249±8
BR(Nπ)	25	32	32	28±3	28±3		40	47	47	45±2	46±2
A _{1/2}	66	64±2	29±3	52±5	52±5		-94	-71±2	-83±4	-71±4	-70±5
A _{3/2}							-121	-92±2	-96±4	-94±5	-93±5

Table I: Properties of selected low-mass nucleon resonances. Breit-Wigner mass, width, and $N\pi$ partial decay width as defined in [9] are given in MeV, the helicity amplitudes in $10^{-3} \text{ GeV}^{-1/2}$.

on the one hand, and BnGa on the other hand: masses, widths and branching ratios are fixed from πN elastic scattering in MAID and SAID. This approach excludes the possibility of photoproduction providing more than the photo-couplings of resonances. Results of the multichannel BnGa-PWA demonstrate however the importance of including information from photon induced and especially double polarization measurements for the determination of nucleon resonance parameters in general.

Finally, we come back to the GDH integral. The contribution of single π^0 production to the GDH integral is evaluated. The total GDH integral up to 2.9 GeV was determined to $I_{\text{tot}}^{2.9} = 226 \pm 5^{\text{stat}} \pm 12^{\text{syst}} \mu\text{b}$ [23–27]; the results were summarized in [3]. Here, a contribution of $27.5 \mu\text{b}$ had been subtracted to account for the description of the very low energy region by MAID [8]. Restricted to a maximum energy of 2.3 GeV, the total integral results in $227 \pm 5^{\text{stat}} \mu\text{b}$ and we find $159 \pm 8^{\text{stat}} \mu\text{b}$ for the contribution of single π^0 production. Up to 0.6 GeV photon energy, this contribution amounted to $156 \pm 8^{\text{stat}} \mu\text{b}$: above $\Delta(1232)$, there is practically no contribution of single π^0 production to the GDH integral.

Summarizing, we have reported the first measurement of the helicity dependent photoproduction cross section for photons at $E_\gamma = 0.6\text{--}2.3 \text{ GeV}$ with nearly full solid angular coverage. The observable E is shown to be highly sensitive to the contributions from s -channel resonances. Even after many years of studying the simplest photoproduction reaction, $\gamma p \rightarrow p\pi^0$, the new data reveal very significant discrepancies in comparison with model predictions. As expected, it is obvious that a fit to differential cross sections and to single polarization observables alone is not sufficient to arrive at unambiguous solutions.

We thank the technical staff of ELSA and the participating institutions for their invaluable contributions to the success of the experiment. We acknowledge support from the *Deutsche Forschungsgemeinschaft* (SFB/TR16) and *Schweizerischer Nationalfonds*.

-
- [1] J. Ashman *et al.*, Phys. Lett. B **206**, 364 (1988).
 - [2] C. Adolph *et al.*, Phys. Rev. D **87**, 052018 (2013).
 - [3] K. Helbing, Prog. Part. Nucl. Phys. **57**, 405 (2006).
 - [4] S. D. Drell and A. C. Hearn, Phys. Rev. Lett. **16**, 908 (1966).
 - [5] S. B. Gerasimov, Sov. J. Nucl. Phys. **2**, 430 (1966) [Yad. Fiz. **2**, 598 (1965)].
 - [6] R. L. Workman *et al.*, Phys. Rev. C **85**, 025201 (2012).
 - [7] R. L. Workman *et al.*, Phys. Rev. C **86**, 015202 (2012).
 - [8] D. Drechsel, S. S. Kamalov and L. Tiator, Eur. Phys. J. A **34**, 69 (2007).
 - [9] A. V. Anisovich *et al.*, Eur. Phys. J. A **48**, 15 (2012).
 - [10] A. Thiel *et al.*, Phys. Rev. Lett. **109**, 102001 (2012).
 - [11] R. L. Workman *et al.*, Phys. Rev. Lett. **110**, 169101 (2013); A. Thiel *et al.*, Phys. Rev. Lett. **110**, 169102 (2013).
 - [12] J. Ahrens *et al.*, Phys. Rev. Lett. **88**, 232002 (2002).
 - [13] J. Ahrens *et al.*, Eur. Phys. J. A **21**, 323 (2004).
 - [14] H. Iwamoto, PhD thesis, GWU, 2011; and AIP Conf. Proc. **1432**, 275 (2012).
 - [15] W. Hillert, Eur. Phys. J. A **28S1**, 139 (2006).
 - [16] H. Olsen and L. C. Maximon, Phys. Rev. **114**, 887 (1959).
 - [17] S. Kammer, PhD thesis, Universität Bonn, 2010.
 - [18] H. Dutz, Nucl. Instrum. Meth. A **526**, 117 (2004).
 - [19] G. Suft *et al.*, Nucl. Instrum. Meth. A **538**, 416 (2005).
 - [20] E. Aker *et al.*, Nucl. Instrum. Meth. A **321**, 69 (1992).
 - [21] R. Novotny, IEEE Trans. Nucl. Sci. **38**, 379 (1991).
 - [22] M. Gottschall, Ph.D thesis, Universität Bonn, 2013.
 - [23] J. Ahrens *et al.*, Phys. Rev. Lett. **84**, 5950 (2000).

- [24] J. Ahrens *et al.*, Phys. Rev. Lett. **87**, 022003 (2001).
- [25] H. Dutz *et al.*, Phys. Rev. Lett. **91**, 192001 (2003).
- [26] H. Dutz *et al.*, Phys. Rev. Lett. **93**, 032003 (2004).
- [27] H. Dutz *et al.*, Phys. Rev. Lett. **94**, 162001 (2005).
- [28] H. van Pee *et al.*, Eur. Phys. J. A **31**, 61 (2007).